

DOI <http://dx.doi.org/10.36722/sst.v10i1.2874>

CFD Simulation and Statistical Analysis of Experimental Designs for Blood Flow in T-Junction Vessels

Cindy Dianita^{1*}, Catherine Nastasya¹¹Process Systems Engineering Laboratory, Department of Chemical Engineering, Faculty of Engineering, Universitas Indonesia, Jl. Lingkar, Pondok Cina, Depok, Jawa Barat 16424.Corresponding author /E-mail: cindydianita@ui.ac.id

Abstract – The blood vessel area that has the greatest chance of atherosclerotic plaque deposition is the bifurcation zone (branching) in the carotid artery. The non-Newtonian fluid of blood has the characteristics of a shear-thinning fluid. Computational Fluid Dynamics (CFD) simulation is used in this study to analyse hemodynamic in carotid artery flow with variations of vessel geometry. The branching geometry of the arteries is represented by a T-junction model which is the ideal simplified blood vessel geometry model to exhibit the most common behaviour in arterial bifurcations. The geometry of the T branch is varied into 4 different combinations of diameter size. Thus, the 2k factorial experimental design method is also used to investigate the effect of the inflow and outflow domain sizes on the response variables in the form of velocity values, Wall Shear Stress (WSS), and Oscillatory Shear Index (OSI). The results of this simulation can greatly help medical scientists to more easily predict areas that have the potential to form atherosclerotic plaques in the circulatory system.

Keywords - Atherosclerotic Plaque, Blood Vessel, Computational Fluid Dynamics Non-Newtonian Fluid, 2k Factorial Method.

INTRODUCTION

The human body has a circulatory system or blood circulation that plays a vital role in distributing nutrients and oxygen to all body parts. Oxygen and nutrients are delivered by transportation in the body called blood. Primarily, blood consists of elements that are formed and suspended in the plasma. The majority of blood-forming element is red blood cells (RBCs). Thus, RBCs are an important component in determining the characteristics of blood flow [1]. Shear-thinning behaviour caused by disaggregation of rouleaux in blood plasma is the leading cause of the behaviour of blood as a non-Newtonian fluid [2]. In addition to the components effect in blood plasma cells, the size of the vascular domain also affecting this behaviour in both medium and large arteries. Furthermore, the viscosity of non-Newtonian fluids also affects hemodynamic factors [3].

Hemodynamic is the movement or blood flow dynamics where this term refers to measurements and general principles that regulate blood flow in the

human body [4]. Locations that have the highest chance of atherosclerotic plaque deposition are the bifurcation zone (branching), curvature in the blood vessels and in areas with low Wall Shear Stress (WSS) values. Stenosis or atherosclerotic plaques blockage that form in the carotid arteries is 80% of the root cause of stroke [5]. In this case, the most established hemodynamic descriptors are velocity, WSS and OSI (Oscillatory Shear Index), where the area with $WSS < 0.5 \text{ Pa}$ and $OSI > 0.2$ is considered a disturbed flow area responsible for the formation of atherosclerosis [6]. In addition to these variables, blood viscosity, blood vessels geometry and systemic blood pressure all play important roles in hemodynamic conditions and atherosclerosis development. Variations in blood viscosity, which can be impacted by factors such as haematocrit levels and plasma viscosity, can have an impact on WSS and contribute to the formation of atherosclerotic plaques. Artery shape, including bends and branches, may lead to obstructed flow patterns and influence plaque formation. Systemic blood pressure affects shear stress and may influence the growth of atherosclerosis.

Many studies related to blood flow through the coronary arteries using different Non-Newtonian viscosity models, namely Power-law, Casson and Carreau model [7]. From several previous studies, it is concluded that the Carreau Yasuda model provides a better estimation than other viscosity models such as Power law and Casson related to WSS in the low to medium shear range [5].

This study is intended to conduct Computational Fluid Dynamics (CFD) simulation to analyse hemodynamic behaviour in carotid artery branching with different geometry of blood vessel. Computational methods such as 3D CFD models can be alternative techniques to in vivo measurement such as MRI to obtain vascular hemodynamic in identifying the risk of plaque destruction [5]. To obtain the effect of the geometry of blood vessel on the hemodynamic, carotid artery is modelled by T-junction with 4 variations of diameter. The T-junction geometric model has been used as a beneficial simplified model to investigate hemodynamic processes both experimentally and conceptually. As the CFD simulation is conducted by varying the diameter of the T-junction blood vessel so that a method is needed to compare multiple experiments in one stage of the process and how they affect each other. Thus, the 2k factorial method is selected, which is a method consisting of k factor where each factor consists.

METHODS

Flow chart of this study is summarized by figure 1 which begins with the collection of blood rheology data and the determination of geometry models. In the next stage, the 2k factorial method is used to create geometry size variations. The 2k factorial design is very useful in the early stages of experimental activity, when numerous factors are expected to be studied [8-10]. Geometries of T branch are diameter variation of 5 mm and 8 mm as shown by figure 2. Geometry creation, meshing and simulation trials are conducted until it reaches convergence. Grid independent test (GIT) is done to get the most accurate mesh values and the shortest

time for research simulations. Hexahedral mesh is used where GIT is performed on the geometry of the first variation with an inlet and outlet the diameter of 5 mm. GIT is performed by comparing the results of different grid numbers that giving relatively stable results of computation with smallest quantity of grids. Denser meshes are often preferred to better capture flow fluctuations. However, a denser mesh with extremely thin computational cells necessitates more computational resources and effort. Thus, it is suggested to pick the mesh with the medium number of cells because to the same numerical findings between medium and fine meshes [11].

Once the geometry with selected mesh type and numbers has been prepared, then the simulation is performed using Ansys Fluent software where the variable response to be taken are velocity, WSS and OSI. Data extraction results are used as input to the statistical software for ANOVA tests in order to obtain the effect of variable factors on variable response. The properties of blood and the simulation parameter are summarized in table 1.

Table 1. Parameter of simulation

Parameter	Input
Model	Solver: Single phase Viscous: laminar
Material	Density: 1.050 kg/m3 Viscosity: 0.0035 kg/s
Operating Condition	1.01325 x 10 ⁵ pa
Boundary Condition	Velocity Inlet: 0.32 m/s Outlet: pressure outlet Wall: no slip boundary condition
Control	Pressure-velocity coupling: SIMPLE Discretization Pressure: second order upwind Momentum: second order upwind
Residual	Absolute criteria Continuity = 0.001 X velocity = 0.001 Y velocity = 0.001 Z velocity = 0.001

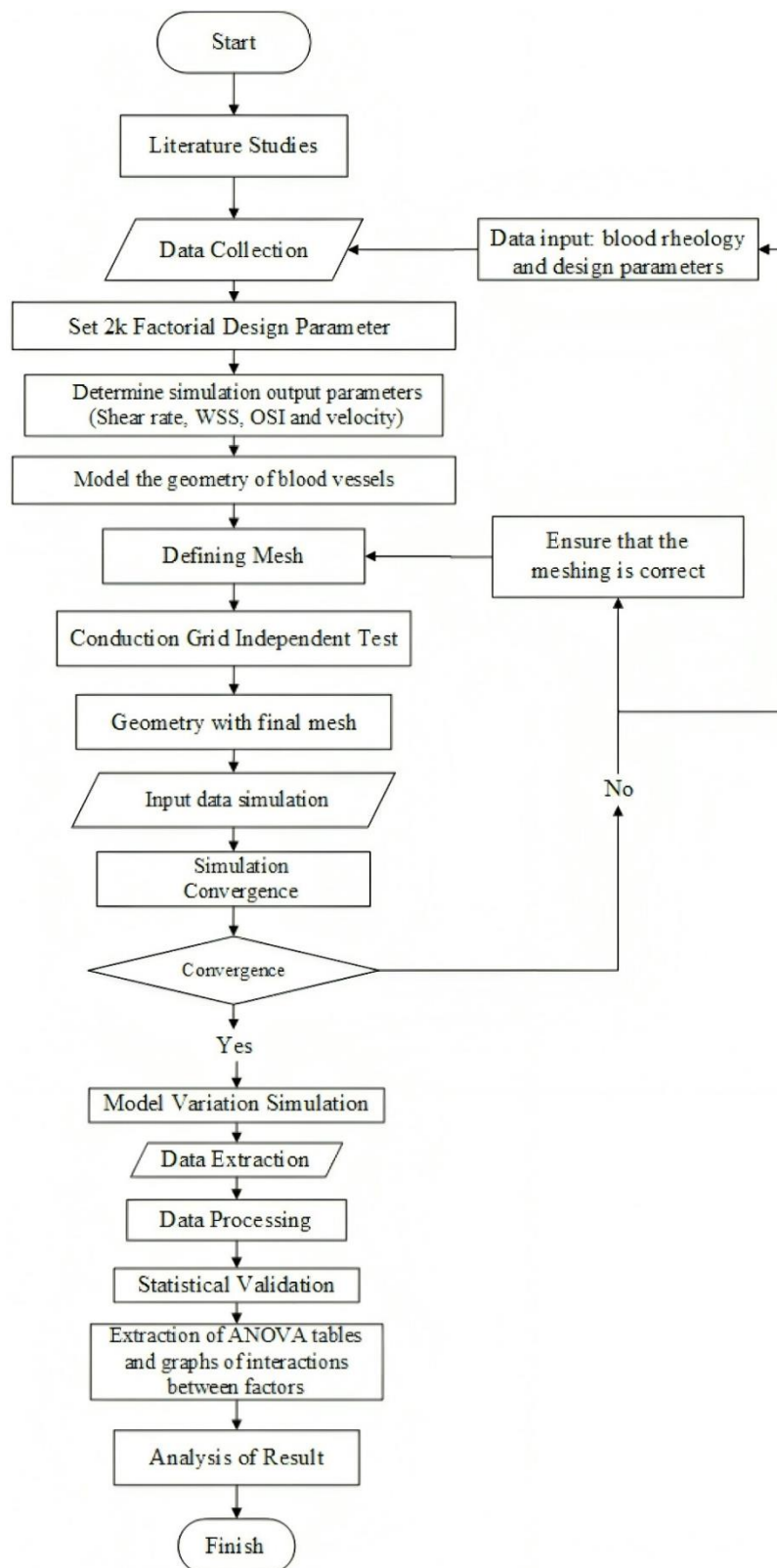


Figure 1. Flow Chart of This Work

RESULTS AND DISCUSSION

As one of the initial steps, GIT is conducted using several mesh variations with an increase in the

number of elements, namely with a range of 80,000 to 500,000 elements. As a result, the design with 450,330 cells is selected as the most optimum quantity of cells. The parameters of mesh quality

(skewness, orthogonality and aspect ratio) are also checked with values located in the range of good quality of mesh requirements.

The design analysis of the 2k factorial experiment was conducted using statistical software. The lowest diameter (5 mm) is coded with “-1” and highest diameter (8mm) is coded with ”1” as summarized in table 2. Post processing activity is dedicated to extract the data of WSS, OSI and velocity data as listed in table 2. In the area near the wall, the flow pattern is disturbed due to various geometric features that influence changes in WSS. WSS is a major vascular flow-related factor responsible for the formation and development of coronary atherosclerotic plaque. Low WSS values also increase atherosclerotic intimal thickness and areas with $WSS < 0.5$ Pa may influence atherosclerotic formation [6], [12]. From the simulation result, 3 geometries indicated the atherosclerotic formation as shown by their WSS values, only geometry of T8-5 shows WSS above 0.5 Pa. Geometry of T8-5 also shows the highest average velocity value.

Another shear stress index that is also studied besides WSS is the oscillatory shear index (OSI) where the OSI distribution has a maximum value in the downstream area of the stenosis/narrowing area. OSI is a dimensionless hemodynamic parameter which is generally used to identify areas that are susceptible to atherosclerosis in blood vessels. OSI represents the oscillatory behavior of shear stress with negative and positive values. At the location of branching or changes in geometry such as narrowing the prevalence of recirculation zones has also been verified where both high OSI, low WSS, and disturbed flow in the section after stenosis/blockage are the main factors that promote the formation of atherosclerotic plaque [13]. Areas with $OSI > 0.2$, are regarded regions with disturbed and detrimental flow patterns and are considered responsible for causing the formation of atherosclerosis [6]. From

the listed results in table 2, all geometry shows OSI values more than 0.2 with smallest similar diameter variation and geometry with enlargement show lower results near to 0.2.

From the WSS, OSI and velocity results, it is indicated that diameter of blood vessel has important roles for the formation of atherosclerosis. Thus, this work uses Variance analysis (ANOVA) to find significant parameters by observing p-values. This analysis is applied to determine the variables that affect the case. Variables consist of the main effect and the interaction effect, where the main effect or effect of a factor is defined as the average change in response resulting from the change in the level of that factor; therefore, it is necessary to evaluate each vital interaction [14]. If the p-value is less than 0.05 (with a confidence interval of 95%), then the parameter significantly affects the response variable.

ANOVA for Velocity

Table 3 shows the ANOVA result when the response variable is the average velocity. As summarized in table 3, it shows that all variable factors inlet diameter (A), outlet diameter (B) and AB interaction and significantly affect the average response velocity. The main effect factors inlet diameter (A) is known to give a positive effect, while the outlet diameter (B) gives a negative effect on velocity. In addition, based on the interaction of AB design parameters, the effect of the inlet diameter (A) is minimal when the value of outlet diameter (B) is at the higher level (coded as “1”) and very large when the outlet diameter (B) is at the lower level (coded as “-1”). According to [6], low-velocity areas are susceptible to the formation of atherosclerosis plaques. Thus, the best geometry approach to geometry that is protective of plaque formation is geometry with inlet diameter (A) at a high level and outlet diameter (B) at a low level.

Table 2. 2k Factorial Design Set-Up

Geometry	Factor 1 Inlet Diameter (A) (mm)	Factor 2 Outlet Diameter (B) (mm)	Response 1 Average velocity (m/s)	Response 2 Average WSS (Pa)	Response 3 Average OSI (-)
T8-8	1	1	0.2707	0.236	0.327
T8-5	1	-1	0.4645	0.634	0.344
T5-5	-1	-1	0.2443	0.216	0.254
T5-8	-1	1	0.2112	0.201	0.256

Table 3. The Analysis of Variance When The Response Variable is Average Velocity

Source	Sum of Square	df	Mean Square	F-value	p-value	
Model	0.0813	5	0.0203	65.20	0.0030	significant
A-Inlet	0.0378	1	0.0078	121.18	0.0016	
B-Outlet	0.0317	1	0.0317	101.83	0.0021	
AB	0.0079	1	0.0079	25.44	0.0150	
Residual	0.0009	3	0.0003			
Cor total	0.0822	7				

Table 4. The Analysis of Variance When The Response Variable is WSS

Source	Sum of Square	df	Mean Square	F-value	p-value	
Model	0.2827	6	0.0471	8545.76	0.0083	significant
A-Inlet	0.0998	1	0.0998	18109.18	0.0047	
B-Outlet	0.1176	1	0.1176	21329.54	0.0044	
AB	0.0608	1	0.0608	11036.62	0.0061	
Residual	5.51E-06	1	5.51E-06			
Cor total	0.2827	7				

Table 5. The Analysis of Variance When The Response Variable is OSI

Source	Sum of Square	df	Mean Square	F-value	p-value	
Model	0.0898	3	0.0299	595.76	<0.0001	significant
A-Inlet	0.005	1	0.005	98.59	0.0006	
Residual	0.0002	4	0.0001			
Cor total	0.09	7				

ANOVA for WSS

Table 4 shows the ANOVA result when the response variable is the WSS average. From table 4, it is known that the variables of factors that have a significant effect are the inlet diameter (A), the outlet diameter (B) and the AB interaction. Referring to [14], if there is an interaction between factors that produce significant effects, then the main effect of such factors should also be considered even though the p-value is above 0.05 (insignificant). From the main effect, it is known that the inlet diameter (A) gives a positive effect, while the outlet diameter (B) gives a negative effect. In addition, based on the interaction of AB design parameters, the effect of the inlet diameter (A) is minimal when the outlet diameter (B) is very large and when the outlet diameter (B) is at the lower level. Regions with low WSS values are susceptible to atherosclerosis. Therefore, large WSS values can be obtained from the approach of geometry with a large inlet diameter (A) and a small outlet diameter (B).

ANOVA for OSI

Table 5 shows the ANOVA result when the response variable is the OSI average. From table 5, it is known that the variable of factors that have a significant effect is only inlet diameter (B). From the main effect, it is known that the inlet diameter (A) gives a positive effect. In addition, there is no interaction

effect that is significant effect of OSI value. OSI values will be high if there are many disturbances or disruptions of flow which is a vulnerable area to plaque formation. Thus, to achieve a flow with a low OSI value, the best approach of geometry is inlet diameter at a low level. According to [7], apart from the influence of cellular components on plasma flow conditions, the size of the flow domain also has an impact on shear-thinning or blood thinning behavior where blood viscosity will become smaller as the diameter decreases.

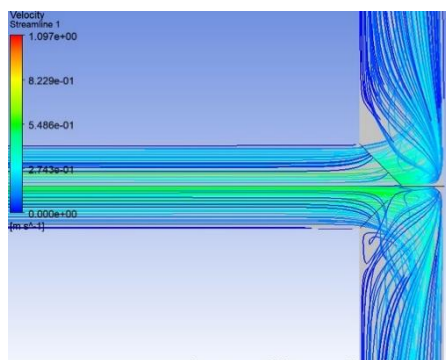
Qualitative Analysis of Velocity Contour

Based on previous study, it is known that differences in the geometric structure of blood vessels, such as the magnitude of diameter and angle of bifurcation, have a significant impact on intravascular flow parameters [13]. Geometric structures affect the slowing and acceleration of fluid particles and support vortex generation in the flow. Bifurcation in blood vessels can increase secondary flow, which affects the rotational movement and transition of blood and builds up low-velocity areas in areas with stenosis [15].

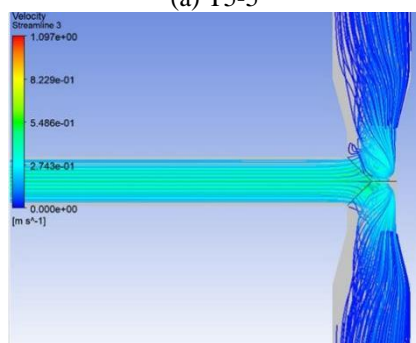
In the model of carotid arteries with T branch, there is a vortex in the junction part (figure 2) where it occurs because the blood flow hits the walls of blood vessels. As a result, reverse circulation is detected

with the area at a low velocity increase. This also happened in each type of geometry in this study but with different intensities caused by differences in geometry size. The recirculation zone supports plaque growth; therefore, T branching geometry is susceptible to atherosclerosis disease. This similar trend is also concluded by [16] who reported that if the branching zone is considered as a transition area with normally a low shear stress area and because low endothelial shear stress is a stimulus for plaque formation and atherogenesis, the branching zones are strong candidates for lesions like atherosclerosis and stenose.

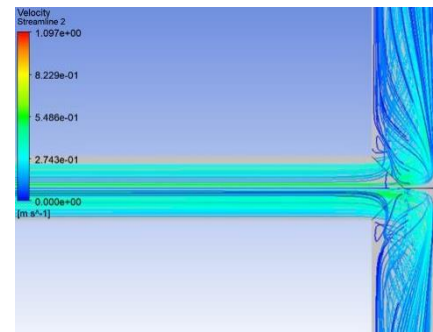
In the body, blood flow generally flows in a laminar manner. However, in high flow conditions, especially in the ascending aorta and carotid artery, laminar flow can transform into turbulent flow. Turbulent flow can also occur in arteries at the point of branching, narrowing or partial obstruction and across stenotic heart valves where turbulence phenomena cause a decrease in flow velocity. Turbulence does not occur until the flow velocity becomes high enough to break the laminar flow. Therefore, when the blood flow velocity increases in the blood vessels, there is no gradual increase in turbulence. Rather, turbulence occurs when the critical Reynolds number (Re) is exceeded [17].



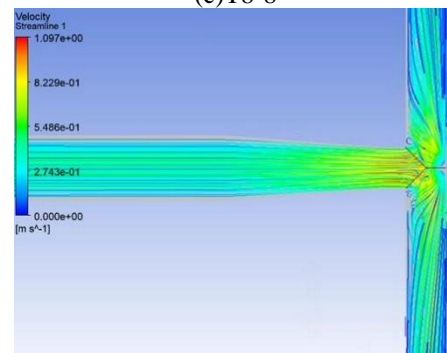
(a) T5-5



(b) T5-8



(c) T8-8



(d) T8-5

Figure 2. Velocity Streamline of Different Geometries of T Branch

Quantitative Analysis of WSS Contour

Areas with low WSS values overlap with the area of flow recirculation [18]. It can be concluded that velocity has a linear effect on the WSS value where this area supports the formation of plaques. Recirculation can be distinguished by zero or negative WSS values where the more blood indicates shear-thinning behavior, the fewer sinus or branching areas undergoing recirculation flow [19]. Thus, it is known that blood vessels with the domain of T branching, both those that experience narrowing, dilation, or with a constant diameter, have a chance for recirculation and flow disturbance where low WSS values are observed in the area indicating that the vascular area has a risk of plaque formation (figure 3).

Quantitative Analysis of OSI Contour

OSI measures the oscillation phenomenon in the WSS vector from the dominant flow direction where high OSI values indicate severe stretching and compression of blood vessel walls causing sufficient damage to endothelial cells and accelerating plaque development [15]. For all geometry of T branch (T5-5, T5-8, T8-5 and T8-8), low OSI values are observed in the domain of blood vessels and show an increase at the downstream of stenosis and bifurcation branching walls where low WSS values also appear, indicating that the vascular region has a risk of plaque formation (figure 4). The formation of

atherosclerosis plaques can occur in low WSS and high OSI regions, so analysis of this region is essential to determine the risk of plaque formation [20]. As captured by OSI contours in figure 4, the contours estimate the similar prediction as shown by the extracted OSI value from simulation as listed in table 2.

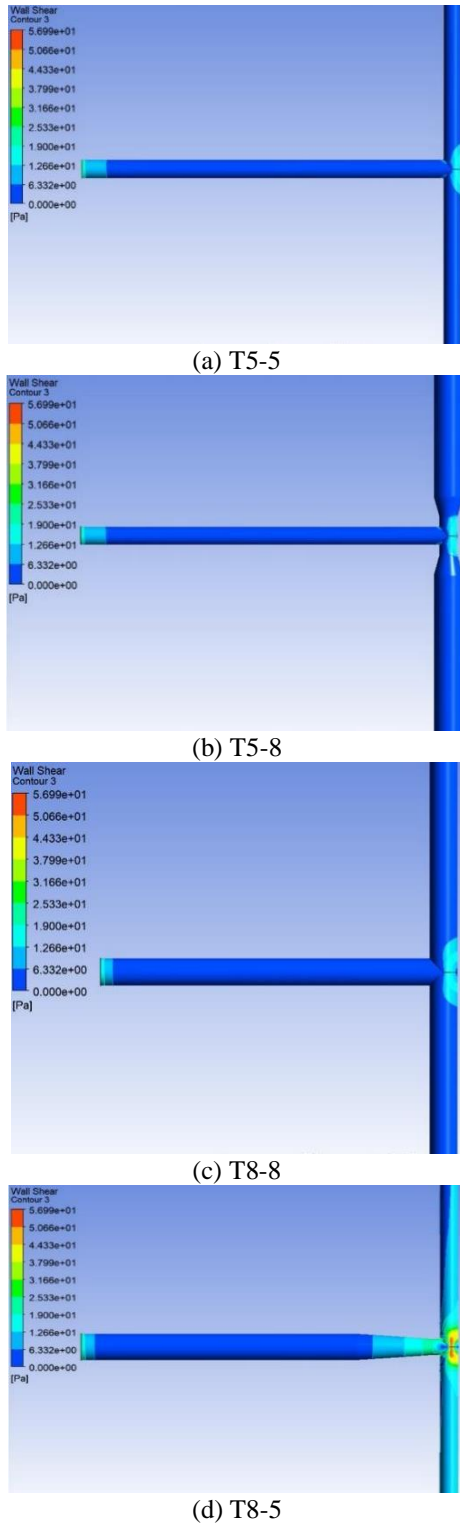


Figure 3. Wall Shear Stress (WSS) Contours of Different Geometries of T Branch

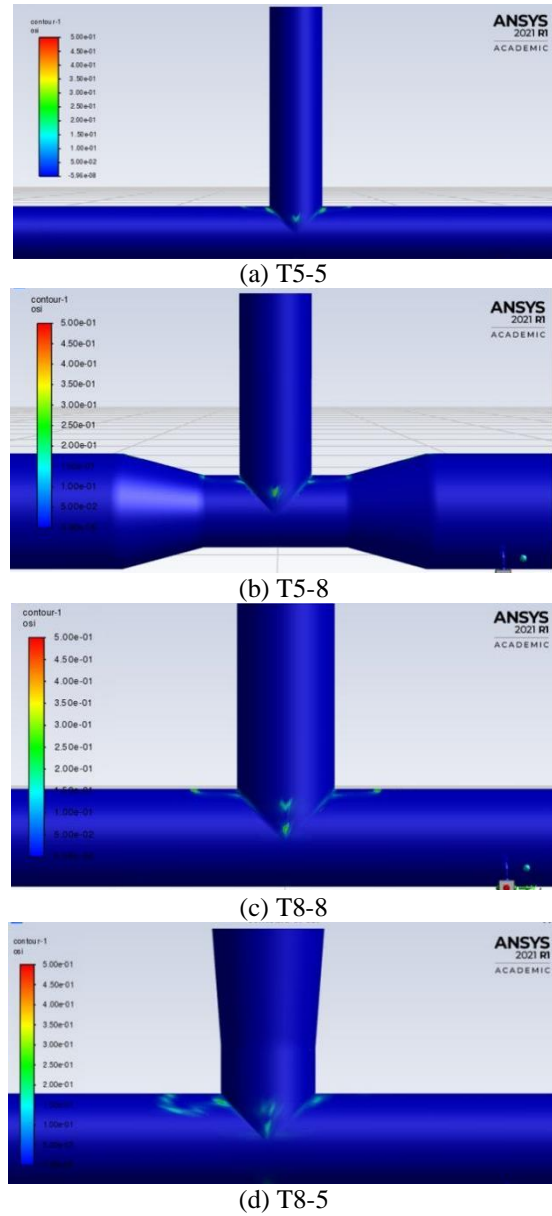


Figure 4. OSI (Oscillatory Shear Index) Contours of Different Geometries of T Branch

CONCLUSION

The simulation used the Carreau-Yasuda model to represent blood as an incompressible, Non-Newtonian fluid with steady, laminar flow and no-slip conditions at the vessel walls. Among the T-junction geometries tested, T8-8 was found to be the most protective against plaque growth.

Simulations of different T-junction designs (T5-5, T5-8, T8-5, and T8-8) showed WSS values ranging from 0.2 to 0.63 Pa, OSI values from 0.25 to 0.34, and velocities from 0.21 to 0.46 m/s. Statistical analysis suggests that geometry with a large input diameter and smaller outlet diameter (T8-5), is best

for reducing plaque risk. This design achieves favorable flow conditions with higher WSS and lower OSI values. However, the qualitative analysis indicates that T8-8 might be better at preventing plaque formation. Future studies should consider additional factors, like the junction angle, to better predict how vessel geometry affects plaque development.

REFERENCE

- [1] M. Renganathan, "CFD simulation of non-Newtonian fluid flow in arterial stenoses with surface irregularities," *World Acad. Sci. Eng. and Technology*, vol. 73, pp. 957–962, 2011.
- [2] R. Chhabra, "Non-Newtonian Fluids: An Introduction," *Rheol. Complex Fluids*, 2010, doi: 10.1007/978-1-4419-6494-6_1.
- [3] A. Chen, A. A. Basri, N. Bin Ismail, and K. A. Ahmad, "The Numerical Analysis of Non-Newtonian Blood Flow in a Mechanical Heart Valve," *Processes*, vol. 11, no. 1, 2023, doi: 10.3390/pr11010037.
- [4] J. Newman, "Hemodynamic," in *Encyclopedia of Behavioral Medicine*, M. D. Gellman and J. R. Turner, Eds. New York, NY: Springer New York, 2013, pp. 955–957. doi: 10.1007/978-1-4419-1005-9_1267.
- [5] N. Kumar, A. Khader, R. Pai, S. Khan, and K. Prakashini, "Computational fluid dynamic study on effect of Carreau: Yasuda and Newtonian blood viscosity models on hemodynamic parameters," *J. Comput. Methods Sci. Eng.*, vol. 19, pp. 1–13, 2018, doi: 10.3233/JCM-181004.
- [6] M. F. Rabbi, F. S. Laboni, and M. T. Arafat, "Computational analysis of the coronary artery hemodynamics with different anatomical variations," *Informatics Med. Unlocked*, vol. 19, p. 100314, 2020, doi: <https://doi.org/10.1016/j.imu.2020.100314>.
- [7] S. S. Shibeshi and W. E. Collins, "The Rheology of Blood Flow in a Branched Arterial System.," *Appl. Rheol.*, vol. 15, no. 6, pp. 398–405, 2005, doi: 10.1901/jaba.2005.15-398.
- [8] C. Dianita, R. Piemjaiswang, and B. Chalermssinsuwan, "CFD simulation and statistical experimental design analysis of core annular flow in T-junction and Y-junction for oil-water system," *Chem. Eng. Res. Des.*, vol. 176, pp. 279–295, 2021, doi: 10.1016/j.cherd.2021.10.011.
- [9] R. Piemjaiswang, Y. Ding, Y. Feng, P. Piumsomboon, and B. Chalermssinsuwan, "Effect of transport parameters on atherosclerotic lesion growth: A parameter sensitivity analysis.," *Comput. Methods Programs Biomed.*, vol. 199, p. 105904, Feb. 2021, doi: 10.1016/j.cmpb.2020.105904.
- [10] T. Yurata, P. Piumsomboon, and B. Chalermssinsuwan, "Effect of contact force modeling parameters on the system hydrodynamics of spouted bed using CFD-DEM simulation and 2k factorial experimental design," *Chem. Eng. Res. Des.*, vol. 153, pp. 401–418, 2020, doi: <https://doi.org/10.1016/j.cherd.2019.10.025>.
- [11] D. Zhao, N. Han, E. Goh, J. Cater, and A. Reinecke, "Chapter 2 - 3D-printed miniature Savonious wind harvester," in *Wind Turbines and Aerodynamics Energy Harvesters*, D. Zhao, N. Han, E. Goh, J. Cater, and A. Reinecke, Eds. Academic Press, 2019, pp. 21–165. doi: <https://doi.org/10.1016/B978-0-12-817135-6.00002-8>.
- [12] T. Asakura and T. Karino, "Flow patterns and spatial distribution of atherosclerotic lesions in human coronary arteries.," *Circ. Res.*, vol. 66, no. 4, pp. 1045–1066, Apr. 1990, doi: 10.1161/01.res.66.4.1045.
- [13] V. Carvalho, D. Pinho, R. A. Lima, J. C. Teixeira, and S. Teixeira, "Blood Flow Modeling in Coronary Arteries: A Review," *Fluids*, vol. 6, no. 2, 2021, doi: 10.3390/fluids6020053.
- [14] R. H. Myers, D. C. Montgomery, and C. M. Anderson-Cook, *Response Surface Methodology: Process and Product Optimization Using Designed Experiments*. Wiley, 2011. [Online]. Available: <https://books.google.co.id/books?id=F6MJJeR2POUC>
- [15] P. Basavaraja *et al.*, "Wall Shear Stress And Oscillatory Shear Index Distribution In Carotid Artery With Varying Degree Of Stenosis: A Hemodynamic Study," *J. Mech. Med. Biol.*, vol. 17, no. 02, p. 1750037, 2017, doi: 10.1142/S0219519417500373.
- [16] T. Sochi, "Fluid Flow at Branching Junctions," *Int. J. Fluid Mech. Res.*, vol. 42, pp. 59–81, 2015, doi: 10.1615/InterJFluidMechRes.v42.i1.50.
- [17] R. E. Klabunde, *Cardiovascular Physiology Concepts*, vol. 3. 2018. [Online]. Available: <http://www.cvphysiology.com/index.html>
- [18] M. Ameenuddin and M. Anand, "Effect of angulation and Reynolds number on recirculation at the abdominal aorta-renal artery junction," *Artery Res.*, vol. 21, pp. 1–8, 2018, doi:

- <https://doi.org/10.1016/j.artres.2017.11.007>.
- [19] M. Toloui, B. Firoozabadi, and M. S. Saidi, “A numerical study of the effects of blood rheology and vessel deformability on the hemodynamics of carotid bifurcation,” *Sci. Iran.*, vol. 19, no. 1, pp. 119–126, 2012, doi:
- <https://doi.org/10.1016/j.scient.2011.12.008>.
- [20] J. Hashemi, B. Patel, Y. S. Chatzizisis, and G. S. Kassab, “Study of Coronary Atherosclerosis Using Blood Residence Time.,” *Front. Physiol.*, vol. 12, p. 625420, 2021, doi: 10.3389/fphys.2021.625420.